X-ray Emission Magnetic Circular Dichroism

R. P. Winarski,[1] P. Ryan,[1] D. Keavney,[1] J. W. Freeland,[1] D. L. Ederer[2]
[1]Experimental Facilities Division, Advanced Photon Source,
Argonne National Laboratory, Argonne, IL, U.S.A.
[2]Department of Physics, Tulane University, New Orleans, LA, U.S.A.

Introduction

Magnetic circular dichroism in x-ray absorption (XA-MCD) has become an impressive technique for examining the magnetic properties of materials [1, 2]. The polarization of the incident radiation and the direction of magnetization of the sample are chosen to selectively excite spin-up or spin-down electrons from core levels into unoccupied states in a material. Differences in the density of spin-up and spin-down states result in a polarization difference in the absorption cross sections. Sum rules can then be applied to these systems to determine the spin and orbital magnetic moments of a material.

A decade ago, it was predicted that x-ray emission magnetic circular dichroism (XE-MCD) should provide information about the spin-resolved density of *occupied* states [3]. Standard x-ray emission spectra measure the local partial density of states (LPDOS), which is the spin-integrated density of states of a particular atomic site of a given angular momentum symmetry chosen according to the dipole selection rules.

In normal fluorescence, x-ray emission can be considered a two-step process. In the first step, an electron is removed from a core level of an atom by external excitation of the sample. In the second step, the created core hole decays when electrons from less-bound levels fill the core hole. This rearrangement of the electrons in the material can result in either radiative or nonradiative transitions.

The fluorescence relaxation process, a radiative transition process, involves the filling of the core holes by electrons in outer electron levels (lower binding energy) or electrons from the valence band. A photon is emitted when an electron fills a hole with an energy corresponding to the energy difference between the level of the core hole and the initial level of the electron making the transition. The emitted photon is then analyzed with a soft x-ray spectrometer.

Analysis of the emitted photons provides data on intensity versus energy distributions that represent the density of the occupied states in a material. When the emission from valence band electron transitions is measured, bonding properties can be deduced from the valence emission spectrum, which is proportional to the density of states.

By measuring samples with circular polarized radiation, with the polarization vector parallel or antiparallel to the applied magnetic field, the spin polarization of the core holes can be selected. Spin is conserved in the dipole transition, so magnetic dichroism in x-ray emission should provide information about spin-resolved LPDOS. The theoretical work has led to several experimental attempts to observe dichroism in emission; however, the measurements made thus far have been hampered by the availability of intense circularly polarized x-rays and have not revealed quantitative LPDOS information [4-11].

Methods and Materials

The soft x-ray emission spectrometer consists of three main elements: an adjustable entrance slit assembly, two spherical gratings, and an area-sensitive multichannel plate (MCP) detector, as shown in Fig. 1. These three elements are positioned on a 5-m-diameter Rowland circle to better than $\pm 5\,\mu m$. Light emitted from the sample passes through the bilateral entrance slit assembly, which can be adjusted from 3 to $1000\,\mu m$ from outside the vacuum system. The instrument employs two spherical gratings — 1200 and 400 lines/mm — which can be independently selected with adjustable beam baffles that either inhibit or allow light that passes through the entrance slit assembly to contact one or both of the gratings. The 1200-lines/mm grating is used to detect emissions between 128 eV (10 nm) and 1240 eV (1 nm), and the 400-lines/mm grating extends the range down to 62 eV (20 nm). The gratings are mounted in holders that allow for adjustments to roll, pitch, yaw, and height and are set for and kinematically mounted inside the instrument. Diffracted light from the gratings is detected with an area-sensitive MCP detector that has its surface tangential to the Rowland circle. The detector moves along the Rowland circle via computerized motor and encoder control to intercept photons of different energies.

When a photon impacts the channel surface of the MCP, several electrons are ejected from the wall of the channel. Because of the presence of an electric field along the length of the channel, these electrons are accelerated until they, in turn, impact the walls of the channel. Since the electrons have gained energy from the field and because of the secondary electron emission coefficient of

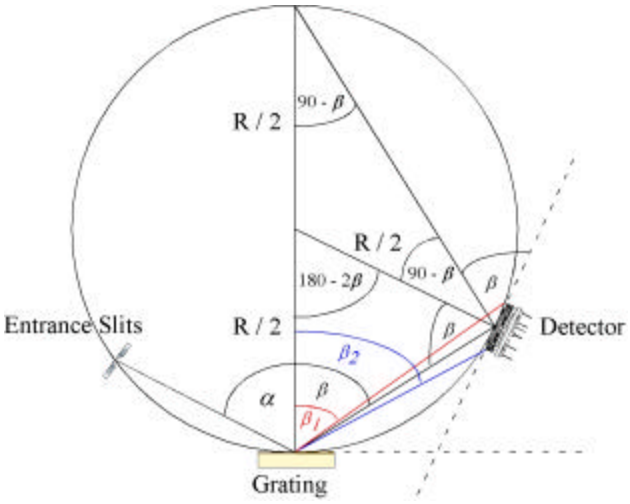

FIG. 1. The three main elements of the spectrometer — the entrance slits, the gratings, and the detector — are precisely located on a Rowland circle geometry.

the channel plate material, each electron causes the ejection of several more electrons from the channel wall. This process repeats, forming an enlarging electron cloud with each impact. A single x-ray photon that strikes a channel of the MCP produces a charge pulse of about 1000 electrons that emerge from the rear of the plate. Since the growing electron cloud is contained within the single channel that the photon impacted, 2-D image information is preserved during the amplification process. The electrons that pass through the plate are collected on a resistive anode encoder (RAE). The RAE consists of a uniform resistive sheet surface with collection electrodes and four conductive contacts at the corners of the anode. The relative charge reaching each of the four contacts from the electrons that pass through the MCPs and encounter the anode is a linear function of the X-Y orthogonal axis position of the RAE. These signals are amplified and processed by an external position-decoding computer and an additional signal-processing computer. Therefore, the impact positions of individual photons can be assigned orthogonal coordinates.

A 2-D image map of the detected emission, as shown in Fig. 2, is processed by computer to correct for distortions from the spherical gratings as well as for variations in efficiency over the surface of the detector. Then counts along the y-axis for each x-axis value are summed to give an intensity versus energy spectrum.

Results and Discussion

Our initial measurements from using the 400-lines/mm grating of the spectrometer have shown a lot of promise. These initial measurements were made with very low signal intensities, since the instrument is designed to

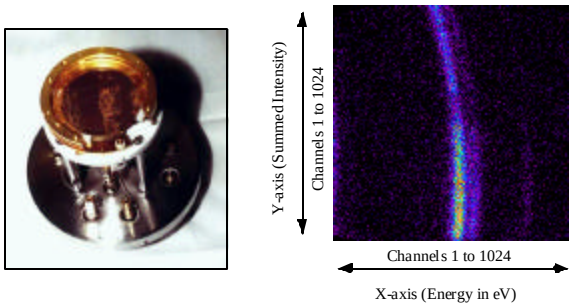

FIG. 2. Photograph of the MCP detector and an image of an accumulated spectrum before it is processed and integrated.

operate with the entrance slits being as close as possible to the emission — normally less than 1 cm from the sample. Under our current configuration, we adapted a chamber that we normally use for absorption and reflectivity measurements to the spectrometer. Unfortunately, this configuration places the entrance slits roughly 11 cm from the sample. So, since our detected intensities were rather low, we were limited to long exposure durations and excitation of the sample above threshold, where we were able to provide a maximum amount of flux onto the sample from our undulator and monochromator. We will receive a new chamber in May 2002 that will optimally position the spectrometer close to the sample. This position will allow us to measure samples by exciting them through and near their absorption thresholds. This capability is important, since recent studies have shown that for this type of experiment, the principal spin-selectivity is achieved by exciting the sample to spin-down (minority) states just above the absorption threshold [11].

Our first measurement from using this technique is shown in Fig. 3. We wanted to detect a dichroic effect in the emission by using the capabilities of our circular polarizing undulator (CPU) and beamline. We found by comparison measurements that our CPU provides greater than 96% polarization, with an incident flux on the sample of about 10^{13} photons/s. X-ray emission spectroscopy (XES) has an advantage over Auger and photoelectron spectroscopies in that these techniques probe only the surface layers of a material. XES can probe thousands of angstroms into a sample, revealing its true bulk properties. In addition, XES provides local information, since it is a core-level spectroscopy, and it is symmetry selective, since it uses the dipole selection rules. An important feature is that because XES involves the detection of photons, strong electrostatic or magnetic fields can be applied to the sample during measurement.

We measured emission from the iron atoms in an iron-nickel alloy buried beneath 280 Å of permalloy. No other technique is capable of measuring these buried layers

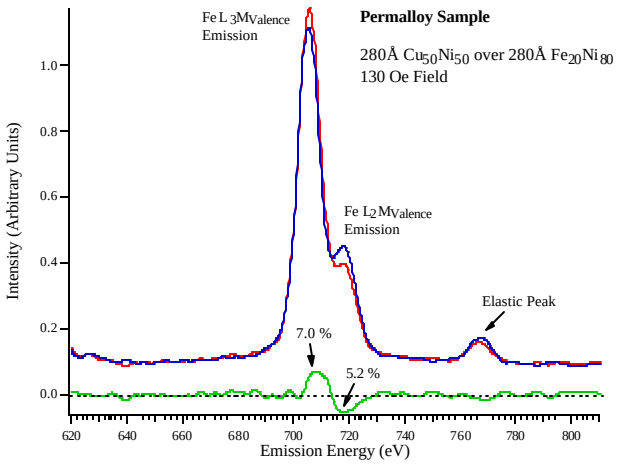

FIG. 3. Emission spectra for right circularly polarized incident radiation (red), left circularly polarized incident radiation (blue), and the dichroism (green).

without destroying the sample in the process. We applied a small electric field of 130 Oe, just enough to switch the magnetization of the iron-nickel layer. The emission spectra were obtained by using the same incident energy on the sample, and, with the spectrometer fixed, changing only the polarization of the incident radiation from right circular polarization to left circular polarization. Dichroism in this sample is clearly evident, with an effect of about 7% for the L_3 emission and about 5% for the L_2 emission.

Note that we used the 400-lines/mm grating, which does not provide enough spectral separation to individually resolve the emission from the filling of the Fe L_2 and L_3 electron levels. We expect to see more features in the dichroism in the Fe L_2 and L_3 emission spectra by using the 1200-lines/mm grating and excitation near the absorption threshold. According to theoretical predictions, the emission dichroism should be on the order of tens of a percent. It is also important to note that since we are not directly measuring the polarization of the emitted photons, this type of measurement must be evaluated with other competing methods of filling the created core holes. Auger and radiative decay filling of the core hole will slightly distort the measured intensities from the emission. In addition, self-absorption effects and dichroic diffuse reflections must be considered [10, 11]. We plan to incorporate corrections for these effects in our future measurements.

Acknowledgments

Use of the APS was supported by the U.S. Department of Energy (DOE), Office of Science, Office of Basic Energy Sciences, under Contact No. W-31-109-ENG-38. This work was supported by National Science Foundation Grant Nos. DMR-9017997 and DMR-9420425 and Experimental Program to Stimulate Competitive Research (EPSCoR)/Louisiana Educational Quality Special Fund (LEQSF) Grant No. DOE-LEQSF 1993-95-03.

References

[1] B. T. Thole, P. Carra, F. Sette, and G. van der Laan, Phys. Rev. Lett. **68**, 1943 (1991).
[2] B. T. Thole, G. van der Laan, and G. Sawatzky, Phys. Rev. Lett. **55**, 2086 (1985).
[3] P. Strange, P. J. Durham, and B. L. Gyorffy, Phys. Rev. Lett. **67**, 3590 (1991).
[4] C. F. Hague, J.-M. Mariot, P. Strange, P. J. Durham, and B. L. Gyorffy, Phys. Rev. B **48**, 3560 (1993).
[5] L.-C. Duda, C. F. Hague, D. C. Mancini, J.-M. Mariot, C. Marliere, J. Nordgren, P. Skytt, and N. Wassdahl, Proc. Mat. Res. Soc. **307**, 111 (1993).
[6] L.-C. Duda, J. Stöhr, D. C. Mancini, A. Nilsson, N. Wassdahl, J. Nordgren, and M. G. Samant, Phys. Rev. B **50**, 16758 (1994).
[7] C. F. Hague, J.-M. Mariot, G. Y. Guo, K. Hricovini, and G. Krill, Phys. Rev. B **51**, 1370 (1995).
[8] L. Braicovich, C. Dallera, G. Ghiringhelli, N. B. Brookes, and J. B. Goedkoop, Phys. Rev. B **55**, R14729 (1997).
[9] L. Braicovich, C. Dallera, G. Ghiringhelli, N. B. Brookes, and J. B. Goedkoop, Solid State Commun. **105**, 263 (1998).
[10] L. Braicovich and G. Ghiringhelli, Phys. Rev. B **58**, 6688 (1998).
[11] S. Eisebitt, J. Lüning, J.–E. Rubensson, D. Schmitz, S. Blügel, and W. Eberhardt, Solid State Commun. **104**, 173 (1997).